



ANALYTICAL FRAGILITY CURVES FOR SKEWED HIGHWAY BRIDGES

Gokhan Pekcan¹ and Ahmed Abdel-Mohti²

ABSTRACT

In this study, the seismic vulnerability of bridges with moderate-to-large skew angles is investigated. The fragility curves are generated using incremental nonlinear dynamic analysis (IDA) of bridges with skew angles of 0, 30, and 60 degrees. The IDA procedure is used with a total of 45 ground motion pairs to develop fragility curves. Damage states are presented and quantified using column rotational ductility and superstructure displacements at the abutments. Furthermore, analytical fragility curves are compared against those recommended by HAZUS. It is demonstrated that as the skew angle increases, skew bridges become more vulnerable to seismically induced damage. It is also shown that the HAZUS fragility curves may not lead to consistent prediction of the vulnerability of skewed bridges.

Introduction

As evidenced in past seismic events (i.e. 1994 Northridge – Gavin Canyon Undercrossing and 1971 San Fernando – Foothill Boulevard Undercrossing), skewed highway bridges are particularly vulnerable to severe damage due to seismic loads. The skew angle plays an important role in increasing the fragility of highway bridges. Therefore, it is important to conduct risk analysis assessment on highway bridges in order to evaluate the amount of damage due to earthquakes.

Bridge damage data immediately after an earthquake serves as invaluable field experimental results (Banerjee and Shinozuka, 2008). Hence, empirical fragility curves can be developed on the basis of real damage data such as those observed after the 1989 Loma Prieta and 1994 Northridge earthquakes. Empirical fragility curves using data from these two earthquakes were proposed by many researchers (Basoz and Kiremidjian, 1997; Der Kiureghian, 2002; Shinozuka et al. 2003; Elnashai et al., 2004). It is noted, however, that empirical fragility curves are highly specific to a particular seismo-tectonic, geotechnical and built-environment. In addition, the observed damage data tend to be scarce and highly clustered in the low-damage and low-intensity range. And because of the high variability of the observational damage classification, empirical fragility curves introduce significant uncertainties. Hence, they may have limited application and may not represent most of the associated uncertainties.

On the other hand, analytically derived fragility curves can be more generic and diverse. Analytical fragility curves are derived based on the damage distributions simulated from numerical/computational analyses. This may reduce the bias and increase reliability of the vulnerability estimate for different structures (Chrysanthopoulos et al., 2000; Mosalam et al., 1997;

¹Assistant Prof., Dept. of Civil and Environmental Engineering, University of Nevada Reno, NV 89557

²Visiting Assistant Prof., Dept. of Civil Engineering, Ohio Northern University, Ada, OH 45810

Reinhorn et al., 2001). They can be developed and used for any class of bridge and/or when real damage data are not available or rare. Development of analytical fragility curves consist of three major steps: (1) simulation or selection of a suitable set of ground motions, (2) nonlinear modeling of bridges, and (3) developing fragility curves from analytical response.

A comprehensive discussion of various alternative methods for constructing fragility curves is given by Porter et al. (2007). There are primarily three different types of analysis commonly used to determine the vulnerability of bridge structures: (1) nonlinear time history analysis (Shinozuka et al., 2000; Hwang et al., 2000a; Karim and Yamazaki, 2001), (2) elastic spectral analysis (Hwang et al., 2000b), or (3) nonlinear static analysis (Mander and Basoz, 1999; Shinozuka et al., 2000). Nonlinear time history analysis is considered to be the most accurate method; however, substantial computational effort is involved. Furthermore, limitations in modeling capabilities as well as the choices of the analysis method, idealization, seismic hazard, and damage models may influence the derived curves and have been seen to cause significant discrepancies in seismic risk assessments. However, the development of fragility curves by analytical means still remains to be the most direct and systematic approach.

The fragility curves presented here were generated using the probabilistic seismic demand model (PSDM) using nonlinear time history analysis. The concept is to relate the engineering demand parameter (or damage indices, DI) to the ground motion intensity (e.g. PGA) using the scaling approach which is known as the incremental dynamic analysis (IDA) (Zhang et al., 2008). Eq. 1 represents the probability of being in or exceeding a given limit state:

$$P[D_I \geq L_{si} | I_M] = \frac{n_i}{N_c} \quad (1)$$

Nonlinear time history analyses are conducted for each ground motion intensity where the damage probability, P is calculated as the ratio of the number of cases, n_i at which the damage index, D_I exceeds or equals the limit state, L_{si} over the total number of cases, N_c for a certain intensity level, I_M (Karim and Yamazaki, 2001).

Damage States

Fragility curves distribute damage among distinct and descriptive damage states. Damages states associated with fragility curves are used along with the corresponding engineering demand and structural response parameters that establish quantifiable damage limits (e.g. drift limits for column, ductility demand on the column, deformation limits at the abutments). Ideally, a survey of experimental and/or post-event field observations is necessary to arrive at consistent definitions and limits. Furthermore, available observed damage data may be used to verify, calibrate and improve the definitions of damage states, hence analytical fragility curves (Banerjee and Shinozuka, 2008).

In most of the published research on the development of fragility curves, deformation limits are established and used for certain components that are identified as the most vulnerable to damage and as critical to the function and structural integrity of the bridge structure. These deformation limits may be associated with column ductility, bearings, hinges, etc. In the present study the rotational ductility of columns (μ_θ) and abutment unseating potential were used to assess the damage states as per Table 1. It is noted that N is the support length measured normal to the center line of the bearing from the edge of the bridge deck to the edge of the abutment. The damage states for column ductility were those proposed by (Choi et al., 2004).

Benchmark Bridge

To achieve the objectives of this study, a highway bridge was chosen from Federal Highway Administration's (FHWA) Seismic Design of Bridges Series (Design Example No.4). The bridge is a continuous three-span box-girder bridge with 97.536 m total length, spans of 30.48, 36.576, and 30.48 m, and 30° skew angle. The superstructure is a cast-in-place concrete box-girder with two interior webs (Fig. 1) and has a width-to-span ratio (W/L) of 0.43 for the end spans and 0.36 for the middle span. The intermediate bents have a cap beam integral with the box-girder and two reinforced concrete circular columns. Reinforced concrete columns of the bents are 1.219 m in diameter supported on spread footings. The longitudinal reinforcing steel ratio of the column is approximately 3% and the volumetric steel ratio of the spirals is approximately 0.8%. Also, the axial load ratio of the column is 14%. The abutments are seat-type with elastomeric bearings under the web of each box girder. In the longitudinal direction, movement of the superstructure is limited by the gap (150 mm) between the superstructure and the abutment back-wall. In the transverse direction, shear keys prevent the movement. This bridge was designed to be built in the USA in a zone with an acceleration coefficient of 0.3g following 1995 AASHTO specifications (AASHTO, 1995). This study investigates the effect of the skew angle on the vulnerability of skewed highway bridges.

Modeling of Bridges

Developing reliable and relatively simple but representative models is the first step in fragility analysis. To develop analytical fragility curves, the benchmark bridge with different geometric configurations with respect to skew angle was selected. Single spine models were developed using SAP2000 (CSI, 2008) and calibrated against 3D FE models of the benchmark bridge. In the models, the superstructure was assumed to be linear-elastic, and all the nonlinearity was assumed to take place in the substructure elements, including bents, external shear keys, bearings, and abutment-soil springs. Table 2 shows the properties of the single spine model. Fig. 2 shows overview of single spine model. The benchmark bridge was altered to produce models with different skew angles (0, 30, 60) and with the same span length. The bridge deck was represented by a single beam element having the equivalent properties of the entire deck. The bents were modeled explicitly; the bent cap was modeled using a 3D frame element with a high moment of inertia to facilitate the force distribution to the columns. Columns and footings were modeled using 3D frame elements. Nonlinearity is assumed to take place in the form of localized plastic hinges at the top and bottom of columns. It should be noted that coupling between moment about the two principal axes was not considered in modeling. Also, the column shear forces remained consistently below the calculated shear capacity for all skew angles (Abdel-Mohti, 2009 and Schroeder, 2006). All footings were assumed to present fixed conditions. Translational and rotational nonlinear spring elements were used to represent the bearings, shear keys, and abutment-soil interaction. Firstly, a preliminary comparative analysis was conducted to assess the accuracy of beam stick (BS) models to capture the response of the finite element (FE) models with skew. For this purpose, the benchmark bridge with 30° skew angle is compared against the more complex finite element model to measure its accuracy. 1940 El Centro ground motion acceleration record was chosen in order to conduct the preliminary time-history analyses to verify the accuracy of the single spine model. A nonlinear static analysis including dead load preceded the time history analyses. A very good agreement between the two models was observed.

Selection of Ground Motions

The benchmark bridge (30° skew) was designed to be built in western USA in a zone with an acceleration coefficient of 0.3g. The PEER Strong Motion Database (<http://peer.berkeley.edu/smcat>) was searched for ground motions with epicentral distances of up to 15 kilometers, Soil-D, and PGA up to 1.0g. A total of 45 ground motions were found and selected for the study, with PGAs ranging from 0.1 to 1.0g. The stronger component of each ground motion was applied in the transverse direction of the three models, while the weaker component was applied in the longitudinal direction. It is noted that no significant effect of orientation of excitation with respect to the skew angle is expected based on the recent study by Schroeder (2006). To conduct the incremental dynamic analyses described earlier, each ground motion pair was scaled to PGAs of 0.1 to 1.0g with increments of 0.1g. It is noted that the stronger components were scaled to the target level first and weak components were scaled by the same respective scale factor. Therefore, a total of 1350 nonlinear time history analyses were conducted using SAP2000 version 12 (CSI, 2008).

Effect of Skew Angle on Fragility

Analytical fragility curves developed for the three bridges with 0, 30, and 60 degree skew are shown in Fig. 3. The development of the fragility curves followed the procedure described in Eq. (1). It is noted that in general if the structural capacity and seismic demand are random variables that conform to either a normal or log-normal distribution then composite performance outcome is log-normally distributed. Therefore, the probabilistic distribution (i.e. fragility) curves are expressed by the two-parameter log-normal cumulative probability density functions. Hence, the cumulative probability of the occurrence of damage, equal to or higher than a given damage state DS, as determined based on Eq. (1) can be fitted to a log-normal cumulative distribution function that is expressed as

$$P[\leq DS] = \Phi \left[\frac{1}{\beta} \ln \left(\frac{x}{\mu} \right) \right] \quad (2)$$

where Φ is the standard normal cumulative distribution function, X is the lognormally distributed ground motion index (e.g., PGA), and μ is the median value of ground motion intensity at which the building reaches the limiting index of damage state DS (Table 1), and β is the standard deviation of the natural logarithm of ground motion index of damage state. The median and standard deviation of the ground motion indices for each damage level were obtained via curve fitting Φ to Eq. (1)

As was mentioned earlier, the system fragility was assessed on the basis of damage to two major components/mechanisms; namely, column rotational ductility and unseating potential at the abutments. Hence, the composite damage states, DS2 through DS5 were quantified as presented in Table 1, such that reaching to the limiting ductility in any one of the four columns or to the limiting superstructure displacement with respect to the abutment (that may lead to unseating) leads to assignment of the corresponding damage state. It is important to note that “100%N” implies complete loss of support at any of the support locations along the abutment.

The fragility curves of the overall system obtained in this study indicate that the bridges with skew are more vulnerable to ground motion effects compared to the regular and straight bridges. As can be seen in Fig. 3, the larger the skew angle is the higher the seismic vulnerability. This observation is valid for all identified levels of damage and at all PGAs, except for DS5 (collapse) at which the

difference between the three fragility curves is not as significant. However, at DS5 level, slightly higher vulnerability of bridges with skew can be seen for PGAs greater than 0.5 g. The primary reason is that the skew bridges experienced higher potential for unseating when subjected to large PGAs (>0.5 g) and unseating followed consistently complete loss of shear keys. This is also attributed to the elevated superstructure rotations about z-axis with skew angle. Although the importance of explicit consideration of skew effects is established, it is also noted that a more refined definition of quantified damage states that also incorporate other bridge components may be necessary.

While the effects of skew on the seismic response of highway bridges are not addressed explicitly in the current AASHTO Specifications (AASHTO, 2007), a skew angle of 20 degrees has been traditionally accepted as the critical angle beyond which special considerations are recommended. Larger deformation demands are recognized for bridges with large skew (> 20 degree). It is worthwhile to note that larger deformations at the skew abutments are expected also due to lower levels of engagement of the soil behind the abutment. This leads to higher potential for unseating when particularly coupled with the superstructure rotations about z-axis. The median PGA values for the four damage states (DS2 through DS5) are summarized in Table 3. These values confirm that the increase in seismic vulnerability becomes more apparent for skew angles greater than 30 degrees.

Comparison with HAZUS Fragility Curves

An early study conducted for the National Institute of Building Sciences developed a document (Basoz and Mander, 1999) which detailed and outlined the steps to conduct fragility curves for use in HAZUS (FEMA, 1999; 2003). The two-parameter log-normal distributions are prescribed with specific median PGAs associated with damage state for various classes of bridges. However, the effect of skew is accounted for using a modification factor ($K_{skew} = \sqrt{\sin(\alpha)}$). Where α is 90 degree for a straight bridge and the skew angle is $(90-\alpha)$. For the continuous bridge considered in the present study, median PGAs of 0.91, 0.91, 1.05, and 1.38 for the four damage states were used in generating HAZUS fragility curves as recommended by Basoz and Mander (1999, Table 18) and FEMA (1999, Table 7.7). Also, soil amplification factors presented in FEMA (1999, Table 4.10) were reported. The recommended standard deviation (SDV), β , for all bridges, is 0.6 based on the study by Mander and Basoz (1999), and later modified to 0.4 in HAZUS-MH (FEMA, 2003).

Fig. 4 presents the generated fragility curves for the bridges with 0° , 30° , and 60° skew using HAZUS method and compares with the analytical fragility curves. For this purpose, analytical fragility curve for 0° skew is used with the modification factor for skew and other applicable factors. It appears that HAZUS underestimates significantly the vulnerability of the class of bridges considered in this study. In other words, the analytical fragility curves predict higher fragilities than those obtained using the HAZUS method. Differences between the analytical and the HAZUS fragility curves may be attributed to the fact that HAZUS methodology is developed using nonlinear static methods, which do not account for the dynamic effects on the overall system response. Also, mechanisms such as; gap opening and closing, pounding, shear key contributions which are expected to affect the dynamic response of the overall system can not be accounted for by means of static methods. Therefore, the response characteristics at the abutments, particularly skew bridge abutments, may lead to larger displacement demands at abutments as well as larger ductility demand on the columns. Therefore, these may lead to the discrepancy between the

analytical and the HAZUS curves.

Concluding Remarks

The effect of skew on the seismic vulnerability of a class of bridge is established through a comprehensive analytical and numerical investigation. Incremental dynamic analysis (IDA) procedure is used to construct the fragility curves for bridges with 0°, 30°, and 60° skew. Two distinct damage mechanisms associated with the column rotational ductility and unseating are considered. The nonlinear time history analyses indicate that skew bridges show higher tendency for unseating primarily due to elevated superstructure rotations about z-axis and lower levels of abutment soil-engagement as the skew angle increases. It is noted that unseating was preceded by the complete loss of shear keys which were modeled explicitly. The effect of skew angle on the fragility of the highway bridges is evident particularly for skew angles greater than 30°. However, analytical fragility curves can be further refined by proper consideration and modeling of possible damage mechanisms that may arise due to soil-foundation-abutment-structure interactions, uplift in the presence of vertical ground motions, etc.

Furthermore, the fragility curves used in the HAZUS methodology underestimate significantly the vulnerability and skew effects. This is attributed to the fact that curves are based on nonlinear static analysis procedures which do not account for the dynamic effects on the overall system response. However, in view of the SDV values recommended by HAZUS and those obtained in the present study, HAZUS fragility curves may be considered as lower bound estimates. Finally, the skew modification factor introduced for use with HAZUS-MH method is found to produce conservative fragility curves when applied to the analytical fragility curves constructed in this study.

Acknowledgment

Partial funding for the study presented in this paper was provided by the California Department of Transportation (CALTRANS) through a contract (59A0503)

References

- Abdel-Mohti, A., 2009, "Seismic Response Assessment and Recommendations for the Design of Skewed Highway Bridges," *PhD Dissertation*, Department of Civil and Environmental Engineering, University of Nevada, Reno.
- American Association of State Highway and Transportation Officials (AASHTO), 1995, "Standard Specifications for Highway Bridges, Division I-A: Seismic Design, American Association of the State Highway and Transportation Officials, Inc.," 15th Edition, as amended by the Interim Specification-Bridges, Washington D.C.
- Banerjee, S., and Shinozuka, M., 2008, "Experimental verification of bridge seismic damage states quantified by calibrating analytical models with empirical field data," *Journal Earthquake Engineering and Engineering Vibration, IEM*, 7 (4), 383-393.
- Basoz, N., and Kiremidjian, A.S., 1997, "Evaluation of bridge damage data from the Loma Prieta and Northridge, CA Earthquakes," The John A. Blume Earthquake Engineering Center, Department of Civil Engineering, Stanford University, *Report No. 127*.
- Basoz, N., and Mander, J.B., 1999, "Enhancement of the Highway Transportation Module in HAZUS," *Report to National Institute of Building Sciences*, Washington, D.C.
- Choi, E., DesRoches, R., and Nielson, B., 2004, "Seismic Fragility of Typical Bridges in Moderate Seismic Zones," *Engineering Structures*, 26, 187-199.

Chryssanthopoulos, M. K., Dymiotis, C., and Kappos, A. J., 2000, "Probabilistic evaluation of behaviour factors in EC8-designed R/C frames," *Engineering Structures*, 22 (8), 1028-1041.

Computers and Structures, Inc., 2008, SAP2000, Version 12.0.1, Integrated Structural Analysis and Design Software, Berkeley, CA.

Elnashai, A., Borzi, B., and Vlachos, S., 2004, "Deformation-Based Vulnerability Functions for RC Bridges," *Structural Engineering and Mechanics*, 17 (2), 215–244.

Federal Highway Administration (FHWA), 1996, "Seismic Design of Bridges, Design Example No. 4 – Three-span Continuous CIP Concrete Bridge," Publication No. FHWA-SA-97-009, October 1996.

FEMA, 1999, HAZUS 99: Technical Manual. Federal Emergency Management Agency, Washington DC.

FEMA, 2003, HAZUS-MH MR1: Technical Manual, Vol. Earthquake Model. Federal Emergency Management Agency, Washington DC.

Hwang, H., Jernigan, J.B., and Lin, Y.-W., 2000a, "Seismic Fragility Analysis of Highway Bridges." *MAEC RR-4*, Center for Earthquake Research Informaion, Memphis, TN.

Hwang, H., Jernigan, J.B., and Lin, Y.-W., 2000b, "Evaluation of Seismic Damage to Memphis Bridges and Highway Systems," *Journal of Bridge Engineering*, ASCE, 5 (4), 322-330.

Karim, K.R., and Yamazaki, F., 2001, "Effect of Earthquake Ground Motions on Fragility Curves of Highway Bridge Piers Based on Numerical Simulation," *Earthquake Engineering and Structural Dynamics*, 30, 1839–1856.

Kiureghian, D.A., 2002, "Bayesian Methods for Seismic Fragility Assessment of Lifeline Components," Acceptable Risk Processes: Lifelines and Natural Hazards, Monograph No. 21, A. Kiureghian, D.A., ed., *Technical Council on Lifeline Earthquake Engineering*, ASCE, Reston VA.

Mander, J.B., and Basoz, N., 1999, "Seismic Fragility Curve Theory for Highway Bridges," *Proceeding of the 5th U.S. Conference on Lifeline Earthquake Engineering*, Seattle, WA, August 12-14, 1999, 31-40.

Mosalam, K. M., Ayala, G., White, R. N., and Roth, C., 1997, "Seismic fragility of LRC frames with and without masonry infill walls," *Journal of Earthquake Engineering*, 1 (4), 693-720.

Porter, K., Kennedy, R., and Bachman, R., 2007, "Creating Fragility Functions for Performance-based Earthquake Engineering," *Earthquake Spectra*, EERI, 23 (2), 471–489.

Reinhorn, A. M., Barron-Corvera, R., and Ayala, A.G., 2001, "Spectral evaluation of seismic fragility of structures, Structural safety and reliability," *Proceedings ICOSSAR 2001*, Newport Beach, CA.

Schroeder, B.L., 2006, "Seismic Response Assessment of Skew Highway Bridges," *M.Sc. Thesis*, Department of Civil and Environmental Engineering, University of Nevada, Reno.

Shinozuka, M., Feng, M.Q., Kim, H., Uzawa, T., and Ueda, T., 2003, "Statistical Analysis of Fragility Curves," *Technical Report MCEER-03-0002*, Multi-disciplinary Center for Earthquake Engineering Research, Sunny Buffalo.

Shinozuka, M., Feng, M.Q., Kim, H.-K., and Kim, S.-H., 2000, "Nonlinear Static Procedure for Fragility Curve Development," *Journal of Engineering Mechanics*, 126 (12), 1287-1296.

Zhang, J., Huo, Y., Brandenburg, S.J., and Kashighandi, P., 2008, "Effects of Structural Characterizations on Fragility Functions of Bridges Subject to Seismic Shaking and Lateral Spreading," *Earthquake Engineering and Engineering Vibration*, 7 (4), pp. 369-382.

Table 1. Definition of Damage Indices and Limit States

Component Damage State	Column Ductility, μ_0	Abutment Unseating Potential
Slight (DS2)	>1	10% N < D < 30% N*
Moderate (DS3)	>2	30% N < D < 50% N

Extensive (DS4)	>4	50% N < D < 100% N
Collapse (DS5)	>7	D > 100%N

* N is the abutment support length

Table 2. Section Properties (FHWA Bridge Example 4)

	Superstructure	Bent Cap Beam	Bent Column
Area (m2)	6.76	2.51	1.17
Ix - Torsion (m4)	10.16	863	0.22
Iy (m4)	3.46	863	0.11
Iz (m4)	83.69	863	0.11
Density (kg/m3)	2915	2402	2402

Table 3. Analytical Median PGAs of Skewed Bridges

Damage State	0-Skew	β	30-Skew	β	60-Skew	β
Slight (DS2)	0.144	0.260	0.138	0.265	0.124	0.290
Moderate (DS3)	0.266	0.290	0.262	0.291	0.245	0.320
Extensive (DS4)	0.520	0.300	0.507	0.310	0.481	0.320
Collapse (DS5)	0.598	0.320	0.595	0.320	0.592	0.350

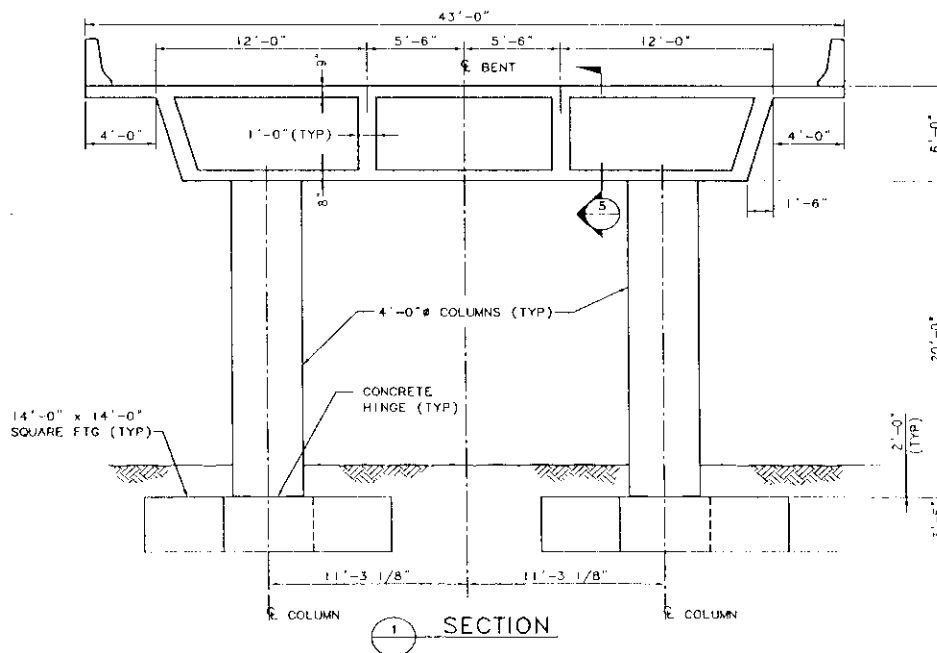


Figure 1. Benchmark Bridge Geometry (FHWA, 1996)

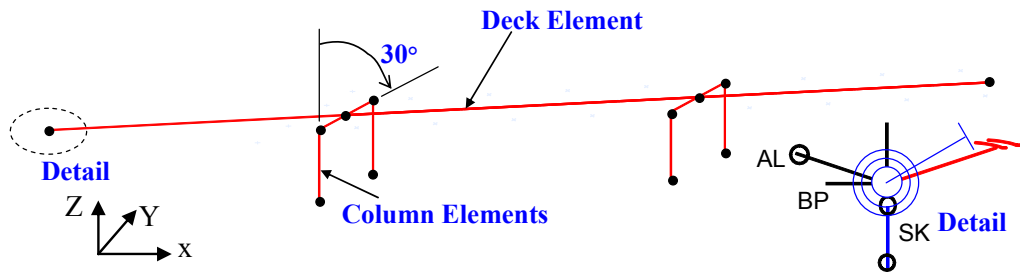


Figure 2. Single Spine Model of the FHWA Example 4 Bridge

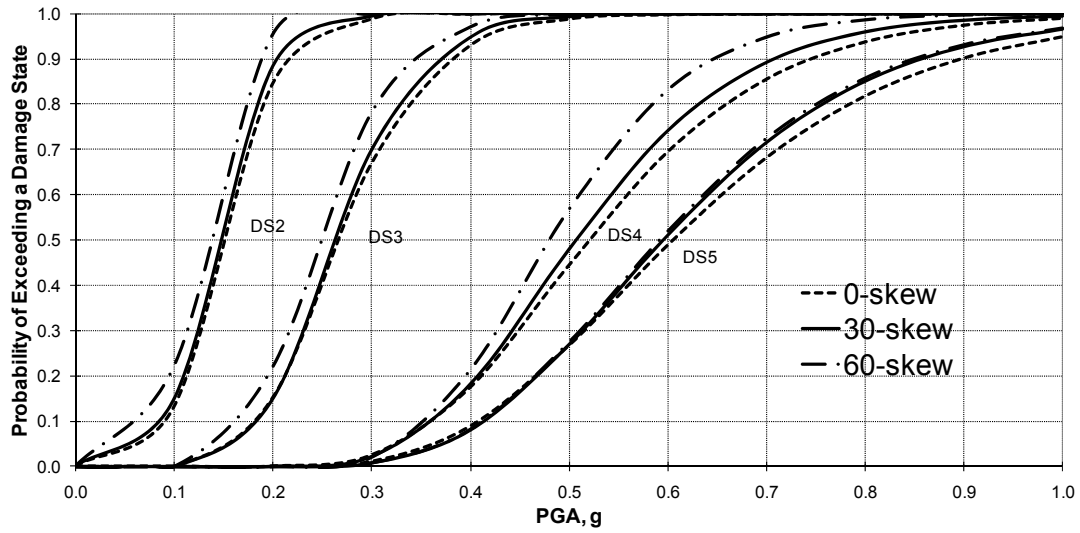


Figure 3. Fragility Curves of Skewed Highway Bridges

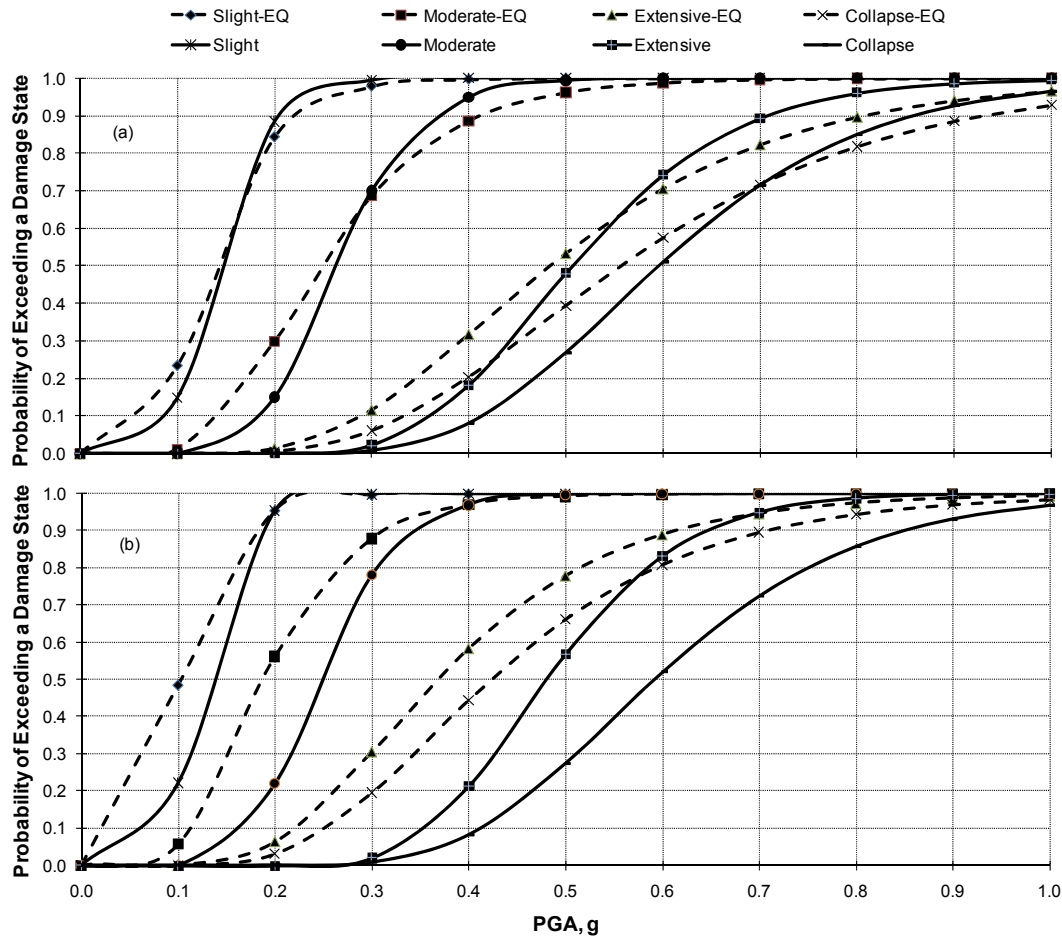


Figure 4. Comparison of Analytical Fragility Curves and Predicted Curves Based on HAZUS Method using Analytical Fragility Curve for 0° (a) 30° and (b) 60°